

Development of High Speed Oblique X-ray CT System for Printed Circuit Board

Atsushi TERAMOTO*, Takayuki MURAKOSHI*, Masatoshi TSUZAKA**, and Hiroshi FUJITA***

The high density LSI packages such as BGA (ball grid array) and CSP (chip scale package) are being utilized in the car electronics and communications infrastructure products. These products require a high-speed and reliable inspection technique for their solder joints. In this paper, we propose the novel oblique CT system that can non-destructively obtain the 3D image representing solder shape of a printed circuit board at a high-speed. This system obtains the projection images from various directions using the rotational flat panel detector and the fixed mounted open-type X-ray generator that has a wide radiation angle, and it obtains the 3D CT image using the 3D FBP (Filtered Back Projection) method. In addition, we developed the CT reconstruction acceleration unit for our CT system, and thus the 3D CT image was obtained in real time. In the experiments, we analyzed the BGA mounted board and the solder crack that is subjected to a thermal shock. These results demonstrated that the proposed system obtained the information that was able to judge the good or defective situation in soldering.

Keywords: X-ray, CT, printed circuit board, BGA and inspection

1. Introduction

Recently, BGA (ball grid array) and CSP (chip scale package)¹⁾²⁾ have been widely used as an LSI package mounted on a PCB (printed circuit board) in electronic products. The electrical junction of the BGA and CSP is formed by solder bumps that are placed in a grid-like formation under the LSI package. The solder shape cannot be observed by optical techniques. X-ray inspection is suitable for the non-destructive inspection of the internal conditions such as the solder shape of the BGA and CSP. Since the advent of BGA and CSP, X-ray inspection has been widely used as the major inspection method of PCBs in consumer electronic products.

With regard to the inspection technique using X-ray fluoroscopy, the authors have developed techniques for extracting the solder using the energy subtraction method³⁾, quantitatively measuring the small solder bump at high speed using the relation between brightness and object thickness in the X-ray image⁴⁾ and detecting microvoids (bubbles) included in a small solder bump by using image data processing and statistical methods⁵⁾. The inspection using X-ray fluoroscopy is suitable for the fast inspection of consumer products because it employs simple mechanics and is able to obtain 2D information from the detector at a time. The X-ray fluoroscopic image, however, is the projection image, and the information in it is compressed along the z direction. Thus, it is impossible to evaluate the 3D solder shape by this technique. In particular, BGA/CSP is being applied to car electronics and communications infrastructure products. Obviously, high reliability is required from these products. In order to meet the inspection requirement for these products, the establishment of the inspection technique which can examine soldered joints more directly is strongly required. In addition, the inspection of the entire shipped product is preferable to guarantee its reliability. To

achieve the complete inspection, rapidity and mechanism assuming the use by the production line are required.

In this paper, we describe an inspection system that can perform accurate and fast inspection of solder junctions in the BGA and CSP for the surface mount process.

X-ray CT technology is a precise technique used for inspecting solder bumps⁶⁾⁷⁾. Several industries use CT to obtain projection data by rotating the sample about an axis that is orthogonal to the axis that connects the X-ray generator to the detector. We call this method vertical CT in this paper. When thin and wide objects, such as PCBs are inspected by the vertical CT, it is necessary to cut out the region of interest of the PCB because it touches the X-ray generator or detector during the scanning process. Since this technique is incapable of achieving non-destructive inspection, it is not used for inspection before a product is shipped but is used for defect analysis during research and development.

To overcome the disadvantages of vertical CT, oblique CT (OCT) was proposed⁸⁾⁹⁾¹⁰⁾, which obtains the projection image of an object from an oblique direction by rotating the X-ray generator and detector. And some systems employed rotation stage and X-ray generator and detector are tilted for the rotational stage. In the OCT, scanning objects move horizontally because X-ray radiation is inclined; thin and wide objects such as PCBs do not touch the X-ray generator and detector. Therefore, although the PCB may be close to the X-ray generator, we can obtain a CT image with high magnification without destroying the PCB.

However, when we introduce OCT to production process, there are three issues. Firstly, it is not possible to achieve the high-speed inspection required in the production process because moving objects (X-ray generator and rotation stage) are very heavy. Secondly, there is problem about the visual field size. The projection images are collected by imaging tube as a 0.3M pixel in the conventional system. The visual field size in OCT image is very small for the size of the entire component at the necessary magnification. There are large gap between inspection time and production cycle in the conventional system. Thirdly is an mechanical adaptaion to production process. Although standard production process requires the PCB transfer system, it is very difficult to introduce to the conventional system structural.

Based on these advantages and disadvantage of conventional

*Nagoya Electric Works Co., Ltd.
550 KATORI, TADO-CHO, KUWANA-CITY 511-0102

**Department of Radiological Technology, Nagoya University
1-1-20 DAIKO-MINAMI, HIGASHI-KU, NAGOYA 461-8673

***Department of Intelligent Image Information, Graduate
School of Medicine, Gifu University
1-1 YANAGIDO, GIFU-CITY 501-1194

(Received January 30, 2007)

OCT, we developed a fast OCT system intended for the online inspection in the production process of BGA and CSP mounted board.

In this paper, the OCT system will be described as follows. In Sec.2, a description of the OCT structure and processing procedure is given. In Sec.3, we show some experimental results. The conclusions are provided in Sec.4.

2. System Description

2.1. Structure and processing outline of OCT

The structure of the OCT system developed by us and the photograph of a prototype system are shown in Fig.1 and Fig.2, respectively. The system consists of a rotational flat panel detector (FPD), an open-type X-ray generator that is set on the elevator and the X-Y stage. The photograph of the FPD and the X-ray generator is shown in Fig.3. By synchronizing the rotation of FPD and the X-Y movement of sample, the X-ray projection images from various directions are obtained.

Unlike the conventional OCT, the X-ray generator needs not rotate because the radiation angle of open-type X-ray generator is 130°. The light weight of the FPD results in a low mechanical load; this further allows high-speed scanning. Regarding to the number of pixels in the projection image, FPD has 5.3M pixel, it is able to obtain the 17 times area for the conventional imaging tube (0.3M pixel).

As described in the previous section, the X-ray generator and the detector do not interfere when the direction of the X-ray irradiation is inclined. The projection image of a thin and wide sample such as a PCB can be obtained under high geometric magnification. The geometrical magnification increases as the distance between a sample and the X-ray generator decreases. The geometrical magnification of the OCT prototype is 200, and a spatial resolution of 0.25 μm is attained at the maximum magnification.

X-ray projection images are transferred to the host memory via image grabber board, and the 3D OCT image is obtained by executing 3D reconstruction on the OCT reconstruction acceleration unit. With regard to the PCB handling, it is automatically inserted and exposed by the conveyor that equipped on the X-Y stage, and the on-line inspection is feasible.

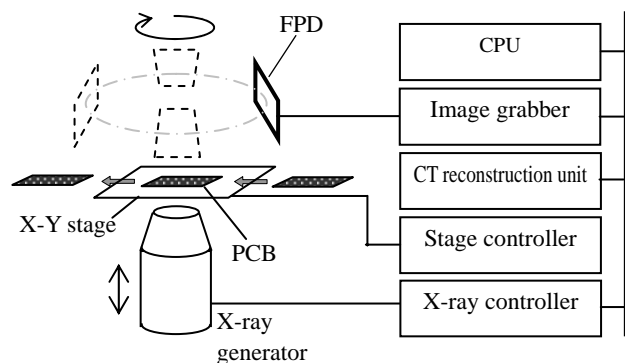


Fig.1 Structure of OCT

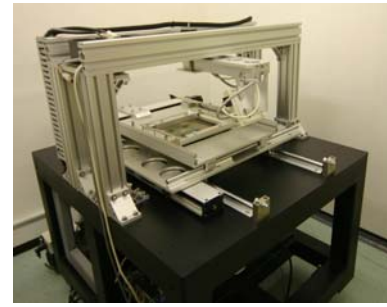


Fig.2 Prototype of OCT

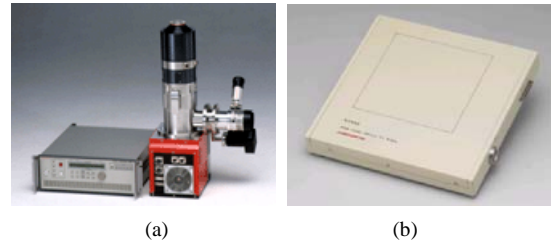


Fig.3 Key components of the OCT such as X-ray generator(a) and flat panel detector(b).

2.2 Data processing

The data processing procedure in the OCT consists of (A) collection of the projection image, (B) image correction, and (C) 3D image reconstruction. This processing is described as follows.

(A) Collection of the projection images

By synchronizing the rotation of FPD and the X-Y movement of sample, the X-ray projection images from various directions are obtained. Here, the center of projection image must keep noticing the identical position while correcting the projection images. The X-Y stage is controlled so that identical position may rotate in radius of gyration RR synchronizing to the FPD as described in Fig.4, and gyration RR is defined as follows.

$$RR = FOD \cdot \tan \alpha \quad (1)$$

where the distance from the X-ray source to the sample is FOD , and the radiation angle of the X-ray source and the detector is α .

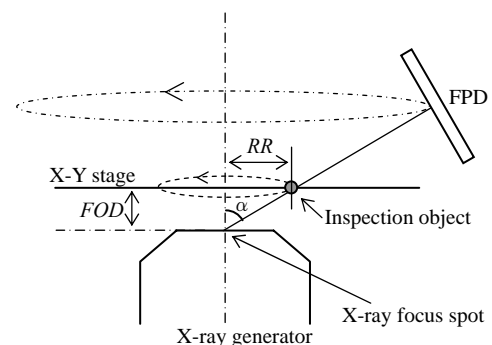


Fig.4 Synchronization of X-Y stage and FPD

(B) Image correction

The projection image have spatial non-uniformity in the proposed system due to the following reasons:

1. The X-ray is irradiated from the focal point of the X-ray generator; the brightest region of the projection image is at the center and the brightness decreases as the distance from the center increases.

2. The focal condition of the X-ray changes with time by thermal change. This results in a change in the distribution of pixel value in the projection image.

To correct the spatial non-uniformity of the image, a non-uniformity corrected projection image $p(m,n)$ is calculated as follows:

$$p(m,n) = -\log_e \frac{I(m,n)}{I_0(m,n)} \quad (2)$$

where $I(m,n)$ is the X-ray intensity of projection, and $I_0(m,n)$ is the X-ray intensity without a sample.

(C) 3D image reconstruction

Fig.5 shows a simplified scheme of the OCT that is equivalent to the scheme in Fig.1. An object $f(\vec{r})$ is illuminated by a cone beam X-ray at the rotation angle ϕ . We assume that \vec{a} and \vec{b} are unit vectors along the horizontal and vertical directions of the detector plane in the 3D space, and \vec{c} is the vector that indicates the direction of projection. The 2D projection $p_\phi(m,n)$ of the object $f(\vec{r})$ is denoted as the integral of $f(\vec{r})$ along the \vec{r} :

$$p_\phi(m,n) = \int_{-\infty}^{\infty} f(\vec{r}) d\vec{r} \quad (3)$$

where \vec{r} is the track from an X-ray generator to the detector, and is defined as $\vec{r} = l\vec{c} + m\vec{a} + n\vec{b}$.

Provided that the X-ray projection is a parallel beam, the 2D Fourier transform $P_\phi(u,v)$ of the projection image is equal to a vertical section of \vec{c} in the 3D Fourier image $F(\vec{\omega})$ based on the projection slice theorem.

$$F(u\vec{a} + v\vec{b}) = P_\phi(u,v) \quad (4)$$

The major methods of image reconstruction from projections are the Fourier method and filtered back projection method (FBP). In this study, we employed FBP to allow high speed reconstruction of 3D images. 3D image reconstruction using FBP is realized by performing filtering and back projection. In the former, a frequency filter $H(u,v)$ is applied to the projection image $P_\phi(u,v)$, as shown in Eq.(5). In the latter, the filtered image $g_\phi(m,n)$ is back projected to the 3D space, as shown in Eq. (6).

$$g_\phi(m,n) = \frac{1}{4\pi^2} \iint P_\phi(u,v) H(u,v) e^{-j(um+vn)} dudv \quad (5)$$

$$f(\vec{r}) = \frac{1}{2\pi} \int_0^{2\pi} g_\phi(\vec{r} \cdot \vec{a}, \vec{r} \cdot \vec{b}) d\phi \quad (6)$$

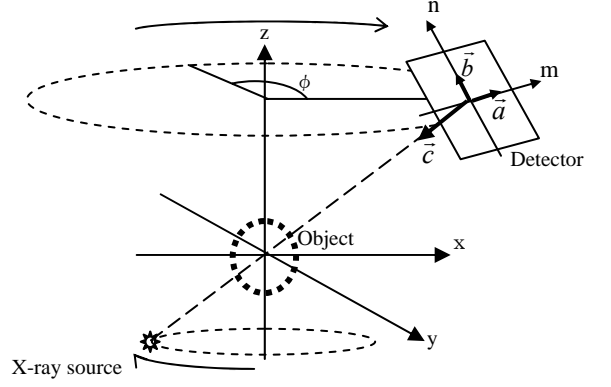


Fig.5 Simplified scheme of OCT

2.3 Acceleration of 3D image reconstruction

In the OCT method, filter processing of the projection images followed by back projection to the 3D space are performed, as described in the previous section. The matrix size depends on the memory buffer size; the maximum size of our prototype system was $2048 \times 2048 \times 32$ at 32 bits per pixel or $2048 \times 2048 \times 64$ at 16 bits. The number of calculations reaches four billion per projection excluding the memory access. Moreover, a large number of random accesses to the 3D memory buffer occur during the back projection processing.

We implemented the reconstruction software on the Windows platform. The processing time is 4.0 s per projection using a dual Xeon 3.6 GHz processor with 4 GB RAM. However, the image acquisition time, including a mechanical movement, is 1 s per projection; the reconstruction is not calculated in real time. To accelerate the reconstruction speed, we developed a CT reconstruction accelerator unit for OCT. **Fig.6** shows the block diagram of the CT reconstruction accelerator unit. It consists of three FPGAs (field programmable gate arrays) with a fast memory buffer connected to each of them, and the projection and 3D OCT images are transferred over the PCI-X slot. The reconstruction time is 0.3 s per projection using this unit, which is 13 times faster than CPU processing.

The acquisition of the projection image and the reconstruction process can be executed in parallel, and the acquisition time is longer than the reconstruction time. Therefore, we can obtain the 3D OCT image in real time.

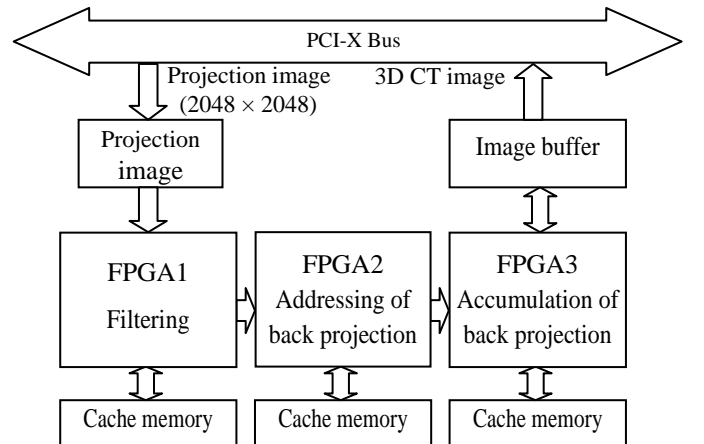


Fig.6 Block diagram of the CT reconstruction accelerator unit

3. Experimental Result and discussion

3.1 Evaluation using BGA mounted board

OCT was applied to the analysis of a BGA mounted board. An evaluation board, on which a plastic BGA with a bump pitch of 1.0 mm and bump diameter of 0.6 mm was mounted were employed. The PCB size was $150 \times 150 \text{ mm}^2$ and the thickness was 2.5 mm. If we had used the conventional vertical CT, we would have had to trim away sections of the PCB except for the analysis region. On the other hand, we did not have to cut any region of the PCB when using the OCT system. Regarding to the inspection speed, projection images were captured at the theoretical limitative speed of FPD, and the reconstruction ended under capturing. As a result, scanning was finished in 32 s. When cycle time of production line is 150 s per board, this system allow to inspect four BGAs without making production line waiting.

Table 1 shows the experimental conditions. **Fig.7** shows the conventional X-ray fluoroscopic image of the BGA mounted board. In this figure, the arrows indicate the soldering defect, and we cannot determine which bump is defective. **Fig.8** shows the horizontal slice image, and **Fig.9** shows the vertical slice image of OCT. **Fig.10** shows the 3D shape of the sample using the volume-rendering technique.

In Fig.8 (b), the bump outline at the defective bump is unclear, which indicates that the solder is not connected correctly between the bump and the PCB. Additionally, Figs 9 and 10 also indicate that some bumps are incorrect at the PCB side.

Table 1 Experimental conditions

X-ray voltage [kv]	100
X-ray current [uA]	100
Matrix size of projection image (X × Y)	2048 × 2048
Matrix size of OCT image (X × Y × Z)	2048 × 2048 × 64
Geometric magnification	10
Spatial resolution (X × Y × Z) [μm]	5.0 × 5.0 × 10.0
Number of projections	32
Inspection time [sec / scan]	32

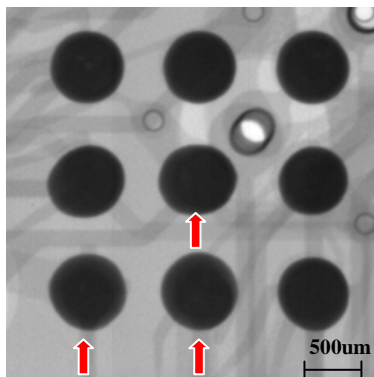


Fig.7 X-ray fluoroscopic image of BGA mounted board

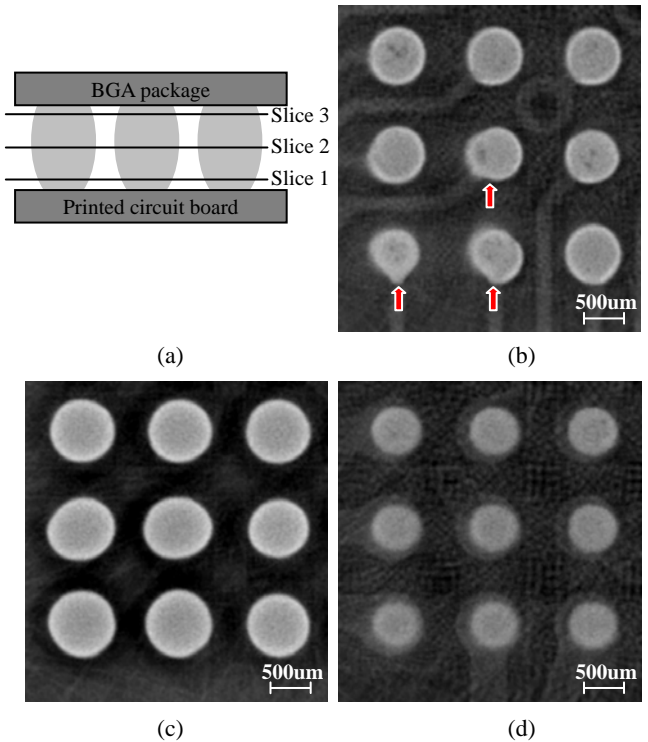


Fig.8 Evaluation result of OCT. (a) illustrates the cross-sectional view of the BGA mounted board and the slice position. (b) to (d) show the horizontal slice image at slice 1 to 3, respectively.

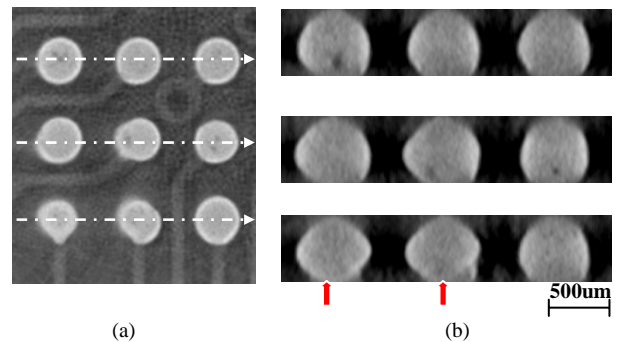


Fig.9 Evaluation result of OCT. (a) is the horizontal slice image which gives the slice line for vertical slice (white arrows). (b) shows the vertical slice images generated from the 3D OCT image along the white lines in (a).

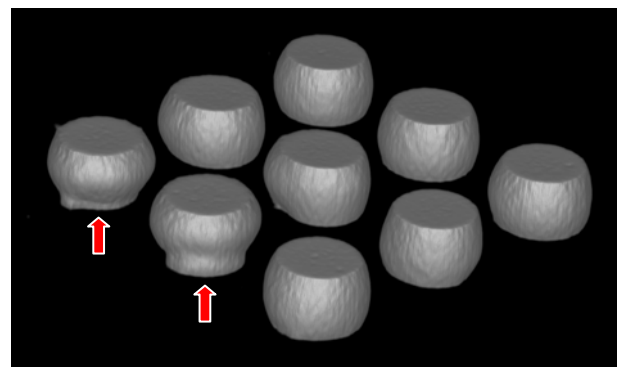


Fig.10 Volume-rendering image

Although most of the solder bumps cannot be observed from the outside, only the outer bumps can be observed using a microscope. To verify OCT, we compared the solder shape in the OCT with that of the microscope. For the evaluation, we used the same conditions as those listed in Table 1. We used VHX-500 (Keyence) as the microscope, and captured the BGA photograph from the outside of the 1.27 mm pitch BGA. The results are shown in Fig.11 (a) and (b). To the right of the bump in Fig.11 (a), solder particles exist under the solder bump, indicating that the solder has not melted. In Fig.11 (b), solder particles also exist on the right hand side. This result demonstrated that OCT can non-destructively analyze the solder shape on the PCB.

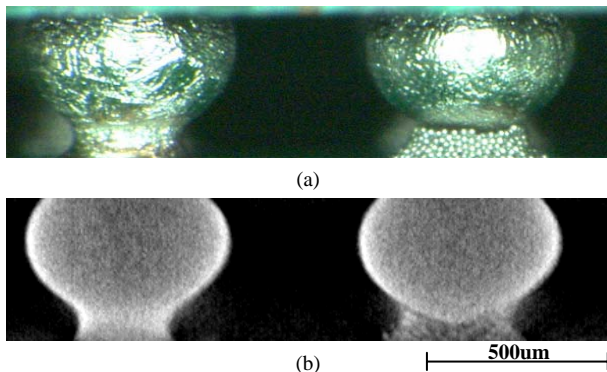


Fig.11 Comparison between photo of microscope (a) and OCT vertical slice image (b).

3.2 Evaluation using chip resistor solder with crack

The generation of cracks due to thermal fatigue and mechanical shock of the solder joint area is a major factor contributing to the decrease in the reliability of electronic equipment, and various researches have been conducted to study solder cracks^{11) 12)}. We evaluated the capabilities of crack analysis using a chip resistor mounted board that was subjected to 3000 cycles of thermal fatigue. The experimental conditions used for the evaluation are shown in Table 2, and the construction of the evaluation board and the OCT images are shown in Fig.12.

Fig.12 (b) is a volume-rendering image of the entire solder shape, and (c)–(e) show the images that sequentially cut it from the solder top to the bottom in the volume-rendering image. The width of the crack was 10~20 µm. This narrow crack can be clearly observed to progress from the surface of the soldering to the inside.

Table 2 Experimental conditions

X-ray voltage [kv]	100
X-ray current [uA]	100
Matrix size of projection image (X × Y)	2048 × 2048
Matrix size of OCT image (X × Y × Z)	2048 × 2048 × 64
Geometric magnification	20
Spatial resolution (X × Y × Z) [um]	2.5 × 2.5 × 5.0
Number of projections	180

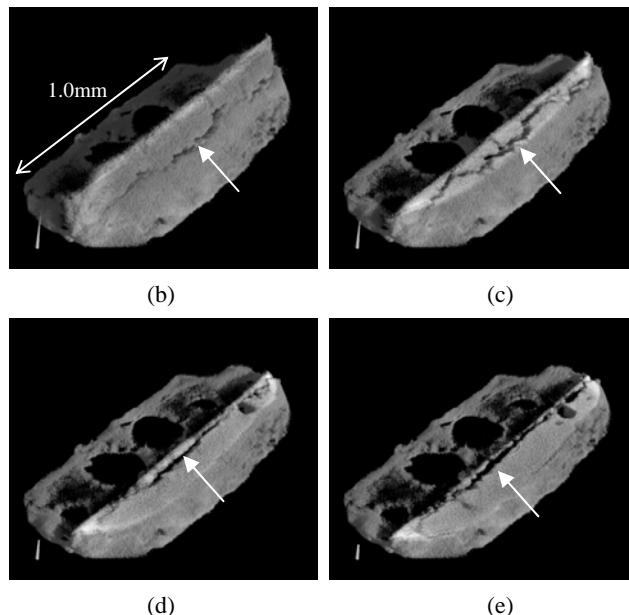
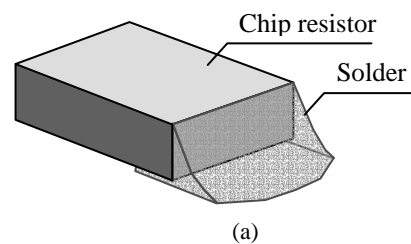


Fig.12 OCT images of solder joint with crack. (a) illustrates the inspection component, (b) is a volume-rendering image of the entire solder shape, and (c)–(e) show the images that sequentially cut it from the solder top to the bottom in the volume-rendering image.

4. Conclusion

In this paper, we proposed a oblique CT system that can non-destructively obtain the 3D solder shape of a PCB at a high speed. This system collects the projection images from various directions using a rotational FPD and a fixed mounted open-type X-ray generator that has a wide radiation angle, and obtains the 3D CT image by the 3D FPB method. In addition, we developed a CT reconstruction acceleration unit for our CT system, and the 3D CT image was obtained in real time. In the experiments, we analyzed the BGA mounted board and solder crack of the chip resistor. The results demonstrated that the proposed system was able to obtain the effective information by non-destructive inspection of the PCB.

Currently, more than 20 inspection systems are operating in domestic and foreign PCB manufacturing factories in order to inspect the BGA solder joint area of car electronics products.

In this paper, we developed the data acquisition system using the OCT system; however, an automated inspection system is required for mass production lines. Presently, we are engaged in the development of an automated algorithm for solder bump inspection.

[References]

- 1) P.Haglund, P.Frisk, J.-O.Andersson : "BGA-MCM technology for harsh environmental applications", ISHM-Europe, 14/16 (1997)
- 2) R.Ghaffarian : "BGAs for high reliability applications", Electronics Packaging & Production, **38-3**, 45/52 (1998)
- 3) A.Teramoto, I.Horiba: "Extraction of Solder Constituent from CSP Boards by Means of X-ray Energy Subtraction Method", Journal of Japan Institute of Electronics Packaging, **4-1**, 68/71 (2001) (in Japanese)
- 4) A.Teramoto, T.Murakoshi, I.Horiba : "High Speed and High Precision Solder Bump Inspection Method Using X-ray Fluoroscopy", IEEJ Transactions on Industry Applications, **125-D-6**, 652/658 (2005) (in Japanese)
- 5) A.Teramoto, T.Murakoshi, Masatoshi Tsuzaka, Hiroshi Fujita : "Automated Detection of Micro Void in Solder Bump", IEEJ Transactions on Industry Applications, **126-11**, 1514/1421, (2006) (in Japanese)
- 6) L.A.Shepp and J.B.Kruskal : "Computerized tomography: The new medical X-ray technology", American Mathematical Monthly, **85**, 655/661 (1979)
- 7) Z.H.Cho : "General views on 3-D Image Reconstruction and Computed Transverse Axial Tomography", IEEE Transactions on Nuclear Science, **21**, 44/71 (1974)
- 8) H.E.Knutsson, P.Edholm, G. H.Granlund, and C.U.Petersson : "Ectomography-A New Radiographic Reconstruction Method-I. Theory and Error Estimates", IEEE Transactions on Biomedical Engineering, **27-11**, 640/648 (1980)
- 9) C.U.Petersson, P.Edholm, G.H.Granlund, and H.E.Knutsson : "Ectomography-A New Radiographic Reconstruction Method-II. Computer Simulated Experiments", IEEE Transactions on Biomedical Engineering, **27-11**, 649/655 (1980)
- 10) H.Matsuo, A.Iwata, I.Hoiba, N.Suzumura : "Three-Dimensional Image Reconstruction by Digital Tomo-Synthesis Using Inverse Filtering", IEEE Transactions on Medical Imaging, **12-2**, 307/313 (1993)
- 11) T.Terasaki, H.Tanie : "Fatigue Crack Propagation Analysis for Micro Solder Joint with Void", Proceedings of 2005 International Symposium on Electronics Materials and Packaging, 37/42 (2005)
- 12) T.Miyazaki, M.Oomiya, H.Inoue, K.Kishimoto, M.Amagai : "Evaluation of Fatigue Strength for Solder Joints after Thermal Aging", Proceedings of 2005 International Symposium on Electronics Materials and Packaging, 215/219 (2005)



Atsushi Teramoto (Member) He received B.S. and M.E. degrees in electrical engineering from Meijo University, Japan, in 1996 and 1998, respectively. In 1998, he joined Opto-electronics division, Nagoya Electric works Co.,Ltd., where he is currently a researcher. His research interests include image processing, image analysis, and image recognition.



Takayuki Murakoshi (Non Member) He received B.S. degree in electrical engineering from Nagoya University, Japan, in 1972. In 1972, he joined Nagoya Electric Works Co.,Ltd., where he is currently a senior researcher. His research interests include data sensing, image processing, and intelligent traffic control system.



Masatoshi Tsuzaka (Non Member) He received the B.S. degree in electrical engineering from Meijo University, Japan, in 1989, and Ph.D. degree from Graduate School of Engineering, Gifu University in 1999. He is currently an Associate Professor in the department of Radiological Technology, Nagoya University School of Health Sciences, Japan. His research interests include the measurement of diagnostic X-ray spectra, study on radiation protection, image evaluation in medicine, computer-aided diagnosis system, tele-Radiology, and high speed networks in medicine.



Hiroshi Fujita (Non Member) He received the B.S. and M.S. degrees in Electrical Engineering from Gifu University, Japan, in 1976 and 1978, respectively, and Ph.D. degree from Nagoya University in 1983. He was a Research Associate at University of Chicago, USA, from 1983 to 1986. He is currently a Chairman and a Professor in the Department of Intelligent Image Information, Graduate School of Medicine, Gifu University, Japan. His research interests include computer-aided diagnosis system, image analysis and processing, and image evaluation in medicine. Dr.Fujita has published over 500 papers in Journals, Proceedings, Book chapters and Scientific Magazines. He is currently a president of Japan Society of Medical Imaging and Information Sciences.